Status and extension of EX-CELO priority project

Zbigniew Piotrowski

September 10, 2019

Original EX-CELO plan

Task 1 - Adaptation of COSMO framework to embrace 0-m level of EULAG DC

- Recoding of boundary conditions and implementation of the diffusion operator into COSMO.
- Research and implementation of physical parameterizations at the surface (i.e. at extra 0 m mass level, or at the 10 m mass level accounting for finite-volume EULAG formulation as opposed to finite-difference Runge-Kutta formulation), including the turbulent surface fluxes.
- Adaptation of COSMO I/O to handle 0 m level.
- Unification of the MPI layer.
- Removal of the COSMO C-grid dependence in COSMO-EULAG.

Task 2 - Enhance the efficiency of COSMO-EULAG algorithms

- Investigation on extending the timestep, e.g. substepping of advection, evaluation of SISL approach
- Adaptive timestep for COSMO-EULAG
- Synchronization with IFS-FVM

Task 3 - Data assimilation capability of COSMO-EULAG

- EnKF capability for COSMO-EULAG

What has been done so far

Task 1 - Adaptation of COSMO framework to embrace 0-m level of EULAG DC - work done

- Recoding of boundary conditions and implementation of the scalar diffusion operator into COSMO. DONE

Task 1 - Adaptation of COSMO framework to embrace 0-m level of EULAG DC - work in progress

- Research and implementation of physical parameterizations at the surface including the turbulent surface fluxes. IN PROGRESS
  1. Successful testing of EULAG explicit diffusion operator for Straka gravity bubble test. DONE
  2. Successful verification of the action of the diffusion operator in curvilinear coordinates. DONE
  3. Use of the EULAG explicit diffusion operator for the real weather simulation (i.e. with space-varying COSMO-computed diffusivity). IN PROGRESS - technical issues
  4. Testing of EULAG dynamical core working on COSMO mass levels vs. COSMO mass levels + extra mass level at 0 m. IN PROGRESS - technical issues
  5. Adaptation of the lower boundary condition of ICON physics to accomodate unstaggered A-grid formulation of EULAG dynamical core. In other words, account for the fact that all variables of EULAG are defined at mass levels and the boundary conditions for dynamics are: no flux for advection, zero vertical velocity at the lowest model level imposed by the iterative solver. IN PROGRESS - minimal COSMO documentation so reverse-engineering needed !!!

Task 1 - Adaptation of COSMO framework to embrace 0-m level of EULAG DC - purely technical tasks

- Adaptation of COSMO I/O to handle 0 m level. Infeasible due to COSMO phase-out
- Unification of the MPI layer. Infeasible due to COSMO phase-out
- Removal of the COSMO C-grid dependence in COSMO-EULAG. Infeasible due to COSMO phase-out

Task 2 - Enhance the efficiency of COSMO-EULAG algorithms

- Investigation on extending the timestep, e.g. substepping of advection, evaluation of SISL approach. DONE
  1. Substepping of the whole dynamics within the timestep of physics successfully done. This enables, for example, integrations of weather at 2 km with dt=80s model timestep. Seems to prevent model crash for solely too large Courant number.
  2. Preliminary test reveal no noticeable negative impact on forecasting scores, more testing is needed.
- Adaptive timestep for COSMO-EULAG. Infeasible due to COSMO phase-out
- Synchronization of algorithms with IFS-FVM. PLANNED
  1. New advection scheme allowing for twice larger vertical Courant numbers.

Task 3 - Data assimilation capability of COSMO-EULAG

- EnKF capability for COSMO-EULAG. Infeasible due to lack of human resources and questionable due to COSMO phase-out. No machine capable to handle operational ensembles at IMGW currently.

Summary and realistic outlook.

- Within the extended EX-CELO timeframe until March 2020, I will continue the attempt to run real weather with EULAG diffusion operator. This may bring substantial changes to the results, as the drag law in EULAG accounts for wind tangent to the slope, not the horizontal wind.
- New MPDATA advection scheme is planned for implementation.
- Further actions are subject to the availability of funding and COSMO-EULAG forecasting scores.

3D scalar diffusion of EULAG

Scalar diffusion in physical (e.g. orthogonal: spherical or Cartesian) coordinates is defined in as a divergence of the Fickian flux of the scalar field, e.g. θ'.

$$\mathcal{H} = \frac{1}{\rho}\frac{1}{\partial \bar{x}^j}\left(\alpha\rho\bar{g}^{jk}\frac{\partial\theta'}{\partial\bar{x}^k}\right) \tag{1}$$

Implementation

Input: scalar field p, kinematic viscosity coeff. *eta*, density *rho*, metric tensor $g11..g33$
Output: scalar field *fp*

Only vertical diffusion evaluation is shown, boundary conditions not shown.

```
gf31=.5*( ( g11(i,j,k+1)*g13(i,j,k+1) + g21(i,j,k+1)*g23(i,j,k+1) )
        +( g11(i,j,k  )*g13(i,j,k  ) + g21(i,j,k  )*g23(i,j,k  ) ) )
gf32=.5*( ( g12(i,j,k+1)*g13(i,j,k+1) + g22(i,j,k+1)*g23(i,j,k+1) )
        +( g12(i,j,k  )*g13(i,j,k  ) + g22(i,j,k  )*g23(i,j,k  ) ) )
gf33=.5*( ( g13(i,j,k+1)*g13(i,j,k+1) + g23(i,j,k+1)*g23(i,j,k+1)
         + g33(i,j,k+1)*g33(i,j,k+1) )
         +(g13(i,j,k  )*g13(i,j,k  ) + g23(i,j,k  )*g23(i,j,k  )
         + g33(i,j,k  )*g33(i,j,k  ) ) )

fz(i,j,k)=((eta(i,j,k+1)+eta(i,j,k))*.5
        * (rho(i,j,k+1)+rho(i,j,k))*.5   )*
          (gf31*( (dxi*(p(i+1,j     ,k+1)-p(i   ,j     ,k+1)))
                 +(dxi*(p(i   ,j     ,k+1)-p(i-1,j     ,k+1)))
                 +(dxi*(p(i+1,j     ,k  )-p(i   ,j     ,k  )))
                 +(dxi*(p(i   ,j     ,k  )-p(i-1,j     ,k  ))) )*.25
          +gf32*( (dyi*(p(i   ,j+1   ,k+1)-p(i   ,j     ,k+1)))
                 +(dyi*(p(i   ,j-j3+1,k+1)-p(i   ,j-j3 ,k+1)))
                 +(dyi*(p(i   ,j+1   ,k  )-p(i   ,j     ,k  )))
                 +(dyi*(p(i   ,j-j3+1,k  )-p(i   ,j-j3 ,k  ))) )*.25
           +gf33*(  dzi*(p(i   ,j     ,k+1)-p(i   ,j     ,k  ))))
...
fp(i,j,k)= fp(i,j,k)+2.*( dxi*(fx(i,j,k)-fx(i-1,j,k))
                         +dyi*(fy(i,j,k)-fy(i,j-1,k))
                         +dzi*(fz(i,j,k)-fz(i,j,k-1)) )/rho(i,j,k)
```

Density bubble

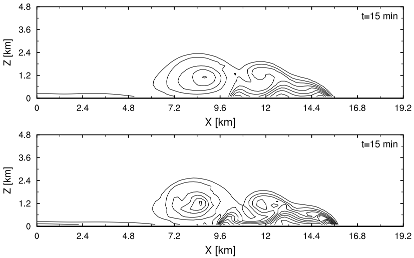

Figure: COSMO EULAG(top) and Runge-Kutta, $dx = 200m$

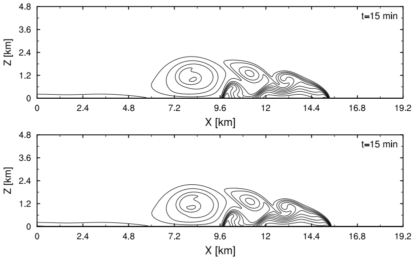

Figure: COSMO EULAG(top) and Runge-Kutta, $dx = 25m$

:

Isolines of potential temperature at 200 m and 25 m for the two dynamical cores are presented after 15 min of simulated time.

Density bubble - difference with COSMO vertical diffusion

Difference in pure EULAG and mixed: vertical COSMO+horizontal EULAG diffusion. Note the different set of variables diffused (T *vs.* θ)

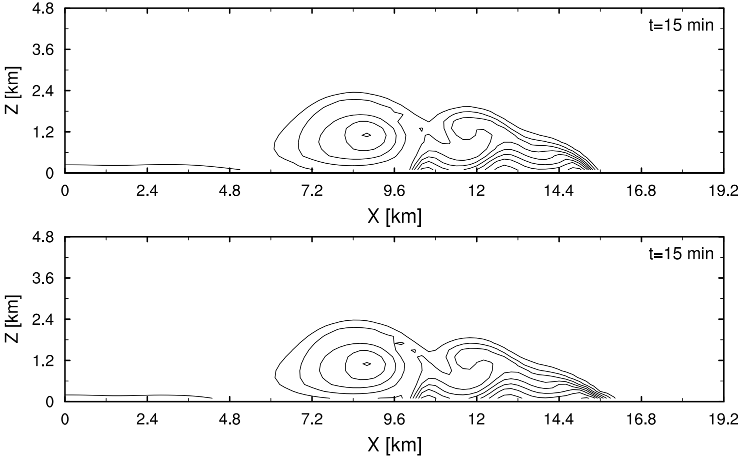

Figure: COSMO EULAG(top) and COSMO-EULAG with COSMO vertical implicit diffusion, $dx = 200m$

Testing implementation of the explicit diffusion operator

Scalar diffusion in physical (e.g. orthogonal: spherical or Cartesian) coordinates is defined in as a divergence of the Fickian flux of the scalar field, e.g. θ'.

$$\mathcal{H} = \frac{1}{\rho}\frac{1}{\partial \overline{x}^j}\left(\alpha\rho\overline{g}^{jk}\frac{\partial\theta'}{\partial\overline{x}^k}\right) \tag{2}$$

Note that proper formulation for momentum is different and it is not yet in the dwarf form/not yet optimized.

- To test the correctness of the operator formulation in curvilinear coordinates, idealized experiment alluding to the water drop evaporation was employed.

Assuming constant diffusion coefficient K, spherical symmetry and initial-boundary conditions $\psi = 0$ for $r > R$ and $t = 0$, $\psi = \psi_0$ for $r \leq R$ and $t \geq 0$, the diffusion process is described by the analytical solution:

$$\psi(r,t) = \frac{R}{r}\psi_0\left[1 - erf\left(\frac{r-R}{2\sqrt{Kt}}\right)\right]_{r\geq R}. \tag{3}$$

The difference between numerical and analytical solution after is presented in Fig. 1 after the three times of characteristic diffusion time (defined as the time at which the flux of substance ψ at $r = R$, integrated over the sphere's surface, is equal to twice its asymptotic value (at $t = \infty$)). Left panel corresponds to the solution in equidistant Cartesian domain, whereas the right panel corresponds to the solution in presence of Gal-Chen coordinate transformation.

Figure: Diff. between analytical and numerical solution for uniform (left) and curvilinear(right) terrain-following grid